




Original Article

Efficacy of Large Groove Texture on Rat Sciatic Nerve Regeneration *In Vivo* Using Polyacrylonitrile Nerve Conduits

ZONGHUAN WANG,^{1,2} YIBING WU,³ YANG XIANG,³ MARIE BEATRIX KRUTH,^{1,2}
PENG WEI,³ GUANGLI DAI,⁴ KEDI XU,^{5,6,7} JUN YIN ^{1,2}
and YONG HUANG⁸

¹The State Key Laboratory of Fluid Power and Mechatronic Systems, School of Mechanical Engineering, Zhejiang University, Hangzhou 310028, China; ²Key Laboratory of 3D Printing Process and Equipment of Zhejiang Province, School of Mechanical Engineering, Zhejiang University, Hangzhou 310028, China; ³Department of Plastic and Reconstructive Surgery, Ningbo First Hospital, Ningbo 315010, China; ⁴Department of Medical Engineering, Ningbo First Hospital, Ningbo 315010, China; ⁵Qiushi Academy for Advanced Studies (QAAS), Zhejiang University, Hangzhou 310028, China; ⁶Department of Biomedical Engineering, Key Laboratory of Biomedical Engineering of Education Ministry, Zhejiang University, Hangzhou 310028, China; ⁷Zhejiang Provincial Key Laboratory of Cardio-Cerebral Vascular Detection Technology and Medicinal Effectiveness Appraisal, Zhejiang University, Hangzhou, China; and ⁸Department of Mechanical and Aerospace Engineering, University of Florida, Gainesville, FL 32611, USA

(Received 1 May 2020; accepted 26 June 2020; published online 15 July 2020)

Associate Editor Xiaoxiang Zheng oversaw the review of this article.

Abstract—Physical guidance cues play an important role in enhancing the efficiency of nerve conduits for peripheral nerve injury repair. However, very few *in vivo* investigations have been performed to evaluate the repair efficiency of nerve conduits with micro-grooved inner textures. In this study, polyacrylonitrile nerve conduits were prepared using dry-jet wet spinning, and micro-grooved textures were incorporated on the inner surface. The nerve conduits were applied to treat 10 mm sciatic nerve gaps in Sprague–Dawley (SD) rats. Sixteen weeks following implantation, nerve function was evaluated based on heat sensory tests, electrophysiological assessments and gastrocnemius muscle mass measurements. The thermal latency reaction and gastrocnemii weight of SD rats treated with grooved nerve conduits were almost 25% faster and 60% heavier than those of SD rats treated with smooth nerve conduits. The histological and immunohistochemical stain analyses showed the repair capacity of inner grooved conduits was found to be similar to that of autografts. These results suggest that grooved nerve conduits with groove width larger than 300 μm significantly improve

peripheral nerve regeneration by introducing physical guidance cues. The obtained results can support the design of nerve conduits and lead to the improvement of nerve tissue engineering strategies.

Keywords—Polymeric nerve conduit, Physical guidance cue, Groove texture, Peripheral nerve regeneration, Dry-jet wet spinning.

INTRODUCTION

Peripheral nerve injury has drawn a lot of public attention, as it drastically affects the quality of patients' lives³ and may lead to life-long disabilities. When large nerve defects (> 10 mm) occur, autografts or allografts are needed to clinically repair the peripheral nerve injury.²⁷ Unfortunately, several drawbacks are associated with these treatments, such as limited levels of donor tissue, donor site morbidity, and mismatching of nerves.³² Nerve conduits represent promising substitutes for autologous nerve grafts.^{43,46} These tubular nerve tissue engineering scaffolds can be designed to incorporate various guidance cues in order to further enhance their repair efficacy.^{15,24,32,44,48}

Recently, different types of contact guidance cues have been applied in nerve conduits.¹¹ The most widely applied guidance structure is longitudinally aligned

Address correspondence to Peng Wei, Department of Plastic and Reconstructive Surgery, Ningbo First Hospital, Ningbo 315010, China. Electronic mail: dr_weipeng@163.com; Kedi Xu, Qiushi Academy for Advanced Studies (QAAS), Zhejiang University, Hangzhou 310028, China. Electronic mail: xukd@zju.edu.cn; Jun Yin, The State Key Laboratory of Fluid Power and Mechatronic Systems, School of Mechanical Engineering, Zhejiang University, Hangzhou 310028, China. Electronic mail: junyin@zju.edu.cn

Zonghuan Wang and Yibing Wu have contributed equally to this work.

microfibers which are inserted into the lumen of the conduits.²⁷ However, these fibers are often non-uniformly distributed. They may also collapse into fiber bundles due to a lack of mechanical support⁴ and hence block the conduit lumen.²² To provide stereologically aligned guidance, the multi-channel structure was incorporated into the nerve conduits. Uniformly distributed channels have been proven to effectively improve peripheral nerve regeneration, however regenerated nerves in individual channels often lack interactions with other nerves,⁴ which leads to impaired recovery and decreased motor function. Moreover, surface topography inside nerve conduits has been utilized to provide contact guidance cues.^{6,10} As one of the most extensively studied contact guidance cues, the longitudinal micro-grooved feature has been widely implemented in nerve conduits. This cue shows to significantly promote *in vitro* neuronal alignment and directional axon outgrowth. Both Schwann cells and PC12 cells have been shown to exhibit improved orientation on grooves with a width of $\sim 10 \mu\text{m}$.^{19,49} Additionally, dorsal root ganglion (DRG) neurons have been shown to exhibit enhanced orientation and extension on poly(lactic-co-glycolic acid) (PLGA) films with incorporated micro-grooves.²⁸ Recently, a number of studies also focused on investigating the application of nerve conduits with aligned inner contours for *in vivo* nerve injury repair and showed promising results for the repair of 10 mm sciatic nerve gaps.^{20,25} The majority of studies, however, focuses on the manufacturing of nerve conduits based on methods which are generally too complex for mass production, such as electrospinning,^{18,36} photolithography³¹ and the rolling-up method.²⁵

In many studies a groove width of only $10 \mu\text{m}$ has been applied for the inner surface area of nerve conduits.^{19,41,49} Notably, this width is significantly smaller than the feature size of nerve fascicles ($> 100 \mu\text{m}$).^{13,52} Additionally, it has been proven that axons are capable of growing across the ridges of neighboring grooves when these have a width of $10\text{--}20 \mu\text{m}$.^{5,28,33,37} Thus, narrow grooves with a width of only $10 \mu\text{m}$ provide limited guidance for axonal outgrowth. Micro-channels with diameters of $200\text{--}300 \mu\text{m}$ have previously been found to effectively guide axons as well as vascular and glial cells inside nerve conduits.^{26,35} To our knowledge, the contribution of micro-grooves with an increased width size ($> 100 \mu\text{m}$) to the *in vivo* recovery of nerve injury has not been investigated. Furthermore, an improved understanding of *in vivo* interactions between nerve tissues and contact guidance grooves is required, as recent studies^{17,41} have mainly focused on the *in vitro* guidance of neuronal behavior.

In our previous studies, we demonstrated that dry-jet wet spinning presents a method that provides high

throughput, precise designs and enhanced control for the fabrication of polymeric hollow fiber membranes that can be applied as nerve conduits. Here, we utilized a micro-structured spinneret to introduce micro-grooved textures into the inner surface area of nerve conduits.^{42,50} In our previous *in vitro* study, we showed that $300 \mu\text{m}$ wide grooves can be applied to guide the axons of PC12 cells to extend along the longitudinal direction of the groove.⁴² This width aligns with the dimension of the sciatic nerve in Sprague–Dawley (SD) rats. In the current study, we prepared semipermeable polyacrylonitrile (PAN) nerve conduits by dry-jet wet spinning and incorporated longitudinal micro-grooved features with a height of $200 \mu\text{m}$ and a width of $300 \mu\text{m}$ into the conduits' inner surface area. The PAN nerve conduits were utilized to bridge sciatic nerve gaps in SD rats, which present an animal model that is commonly used for peripheral nerve injury.¹² This study evaluated the *in vivo* repair efficacy of the grooved conduits in the treatment of rat sciatic nerve damage. Repair was evaluated based on behavioral, electrophysiological, histological and immunohistochemical tests. The aim of this study was to provide a promising method for the manufacturing of nerve conduits with a micro-grooved topography for contact guidance of regenerated nerves. Furthermore, we aimed to investigate the mechanisms involved in *in vivo* interactions between nerves and micro-grooved patterns.

MATERIALS AND METHODS

Preparation and Characterization of Nerve Conduits

Nerve conduits were prepared with the dry-jet wet spinning method^{29,50} as shown in Fig. 1. The dope fluid was prepared by dissolving PAN (MW = 150 kDa, Sigma, US) in dimethyl sulfoxide (DMSO, Sigma, USA) with a weight concentration of 9% (w/w). Deionized (DI) water was used as the nonsolvent and coagulant. The dope and the bore fluids were pumped into the spinneret and the hollow fiber membranes were formed due to phase inversion. Following fabrication, the generated hollow fiber membranes were washed with DI water for 2 h and subsequently left inside DI water for an additional 48 h to allow for residential solvent to be fully removed.^{47,50} The hollow fiber membranes were then applied as nerve conduits. The cross-sectional morphology of nerve conduits was observed with a light microscope (AZ100, Nikon, Japan). The morphology of the nerve conduits was observed with a scanning electron microscope (SEM, SU-8010, Hitachi, Japan). Before the SEM observation, the conduit samples were air-dried in the desiccator for 12 h and then coated with 30-nm gold.

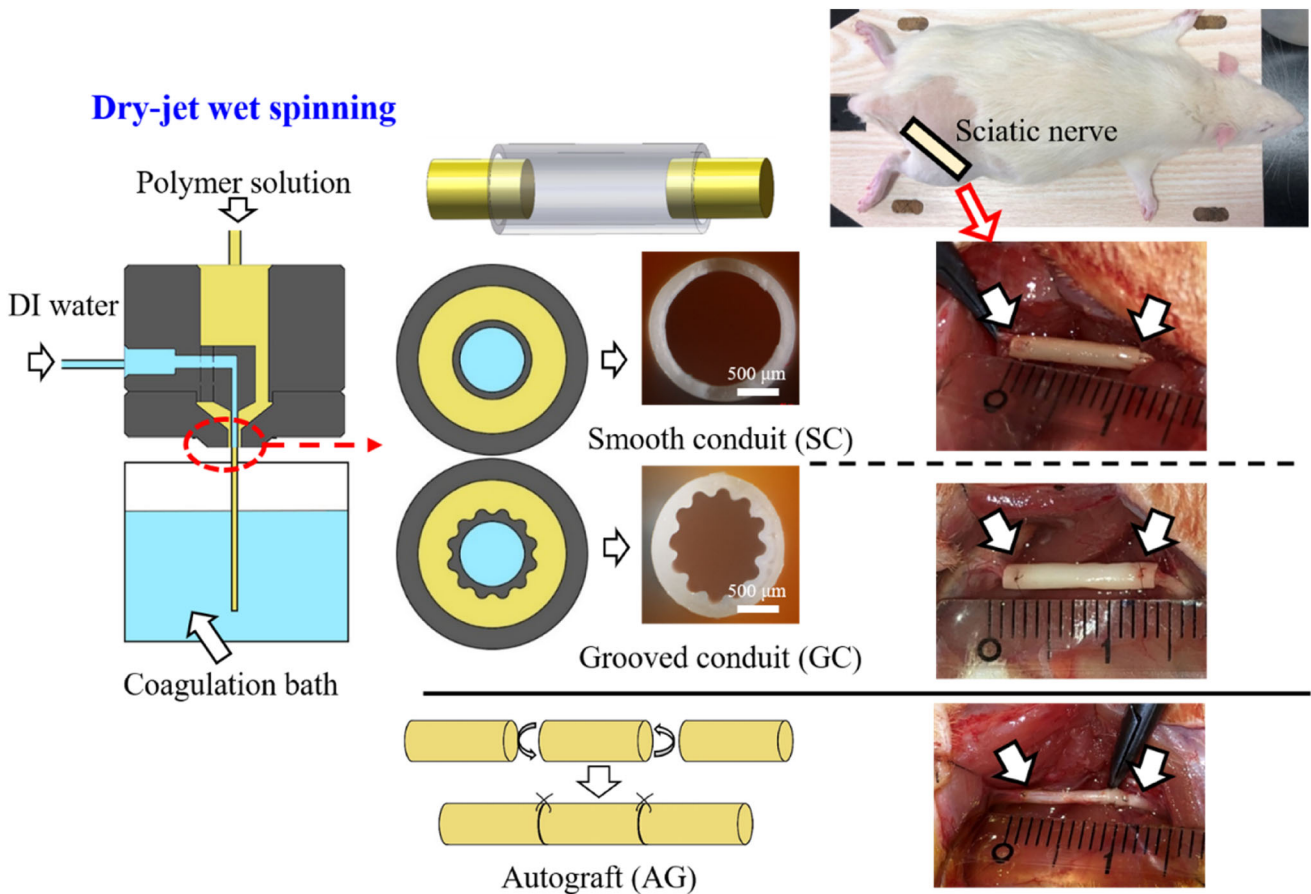


FIGURE 1. Schemes of the nerve conduit fabrication and rat sciatic nerve repair experiments.

During SEM observation, the extra-high tension acceleration voltage (ETH) was set as 3 kV. The definition of groove height and groove width of the nerve conduits were described in our previous studies.⁴²

The overall porosity of PAN nerve conduits was obtained by

$$f_p = \left(1 - \frac{\rho_{\text{conduit}}}{\rho_{\text{PAN}}}\right) \times 100\%, \quad (1)$$

where ρ_{PAN} (1.184 g/cm³) is the density of pure PAN, and ρ_{conduit} is the density of PAN nerve conduits acquired from

$$\rho_{\text{conduit}} = \frac{4m}{\pi(\text{OD}^2 - \text{ID}^2) \cdot l}, \quad (2)$$

where l and m are the length and mass of the PAN nerve conduit, respectively, and ID and OD are the inner and outer diameter of the nerve conduit.

Animal Implantation of PAN Nerve Conduits

The experimental paradigm was designed and implemented as shown in Fig. 1. All procedures performed in

this study were in accordance with the guide for the care and use of laboratory animals (China Ministry of Health) and the protocols approved by the Zhejiang University Animal Care and Use Committee. Male adult SD rats, weighing 350 ± 50 g, were randomly divided into 3 groups ($n = 8$ in each group): the smooth conduit group (SC), the grooved conduit group (GC) and the autograft group (AG). Each rat was anesthetized, and the right sciatic nerve was exposed using the blunt splitting method to remove a 10-mm long nerve segment. In the AG group, the removed nerve segment was then reversed by 180° and re-implanted into the gap with 9-0 microsutures (0.03 mm diameter, Lingqiao Suture, Ningbo Medical Needle Co., Ltd.). In the nerve conduit groups, the gap was bridged with a 12 mm nerve conduit. 1 mm of the proximal and distal nerve stumps was inserted into the conduit and then sutured to the conduit wall with 9-0 microsutures. The wound was then closed in layers using 4-0 sutures (0.15 mm diameter). It is noticed that only the right sciatic nerve received the operation with a conduit or an autograft in each rat, the left sciatic nerve was left unoperated as the healthy group. The animals were housed in temperature-controlled (25 °C) rooms with 12-h light cycles.

Thermal Stimulation Tests

A single, blinded thermal stimulation test was performed on SD rats every 4 weeks after the surgery.²³ In each group, 8 rats were tested in experiments. Rats were placed on a wire net platform in a transparent chamber and left for habituation for 5 min prior to the experiment. A heat source of 60 °C was placed under the healthy and operated hind paws of the rats with a maximum limit of 20 s, and the time needed for rats to withdraw the hind paw was recorded. Each rat was tested 3 times with 5-min interval between tests.

Electrophysiological Tests

Electrophysiological assessments were performed at 16 weeks post operation. In each group, 8 rats were randomly selected for the electrophysiological experiments. Each rat was anesthetized, and the sciatic nerve was re-exposed. The ends of a bipolar hook-like stimulating electrode were placed under the sciatic nerve at the proximal ends of the nerve conduit. A needle-like recording electrode was inserted into the gastrocnemius muscle. The sciatic nerve was stimulated with a mater-8 stimulator (A.M.P.I., Israel) at 0.1 mA for 0.1 ms. The compound muscle action potentials (CMAPs) were recorded with the PowerLab System (PowerLab System, ADInstruments Pty. Ltd.). The motor nerve reaction latency and the peak amplitude of the CMAPs were then calculated.^{1,34}

Gastrocnemius Recovery Evaluation

All the gastrocnemii samples (8 rats in each group) were harvested for evaluation. Both the operated and healthy sides of the SD rats' gastrocnemius muscles were removed and weighed to assess the extent of atrophy caused by denervation. Gastrocnemius muscles were fixed in 4% paraformaldehyde, embedded in paraffin, and cut into 5 μm -thick transverse sections. The sections were then stained with the Masson's staining method to discriminate between collagen and muscle fibers. The stained sections were observed and imaged with light microscopes (IX81, Olympus, Japan). The areas covered by muscle fibers (A_{muscle}) and collagen fibers (A_{collagen}) were estimated with the ImageJ software (<https://imagej.nih.gov/ij/>),²³ and the area percentages of the two fibers was defined as $\varphi_{\text{muscle}} = A_{\text{muscle}} / (A_{\text{collagen}} + A_{\text{muscle}})$ and $\varphi_{\text{collagen}} = A_{\text{collagen}} / (A_{\text{collagen}} + A_{\text{muscle}})$.³⁰

Histological and Immunohistochemical Evaluation

At 16 weeks post operation, the rats were euthanized and regenerative nerves were harvested. Five

specimens from each group were fixed in 4% paraformaldehyde and embedded in paraffin. The middle portions of the specimens were cut into 5 μm -thick transverse sections. The sections were then stained with hematoxylin and eosin (H&E). The stained sections were observed with a light microscope, and the area of nerve fiber cross sections was measured with ImageJ.¹⁶

For the immunohistochemistry analysis, 5 μm -thick transverse sections were maintained in xylene for 2 h and then washed with ethanol. Nerve slices were incubated in goat serum at room temperature for 20 min after which serum was removed. To visualize the growth patterns of nerve fibers, tissue slices were subjected to immunofluorescence staining. The nerve axons were detected with the anti-neurofilament 200 antibody (Anti-NF200, Hebei Bio-high technology), while the Schwann cells were detected with anti-gial fibrillary acidic protein (Anti-GFAP, Hebei Bio-high technology). The nerve slices were kept in 37 °C for 20 min and then fixed with resins. The stained sections were observed with a light microscope and NF200- and GFAP-positive areas were measured with the ImageJ software.

Transmission Electron Microscopy (TEM) Examination

In order to observe the detailed structure of the axons and myelin sheaths of the regenerated nerves inside the nerve conduits, TEM examinations were carried out. Here, five specimens from each group were fixed in 2.5% glutaraldehyde dissolved in phosphate buffer (PBS, 0.1 M, pH 7.0). The specimens were washed three times with PBS, postfixed with 1% OsO₄ dissolved in PBS and then washed again with PBS. Subsequently, the specimens were dehydrated with a graded ethanol series and embedded in resin. The embedded specimens were sectioned using the LEICA EM UC7 ultratome and sections were stained with uranyl acetate and alkaline lead citrate for 5 and 10 min, respectively. The stained sections were then observed with a Hitachi Model H-7650 Transmission electron microscope. Five middle-powered fields ($\times 5000$) in each section were randomly chosen for the quantitative analysis. The thickness of the myelin sheaths and G-ratios (ratio of the axon diameter to the fiber diameter)⁵³ were analyzed using the ImageJ software.

Statistical Analysis

SPSS 21.0 were used for the statistical analysis. Data was expressed with the mean \pm standard deviation (SD). Data of at least five specimens from each

group were included in the statistical analysis. Statistical significance was identified with the one-way ANOVA test. p -values of < 0.05 were considered statistically significant.

RESULTS

Nerve Conduit Characterization

Cross-sectional and surface images of the developed smooth and grooved nerve conduits were shown in Fig. 2. The macro- and micro-dimensions of nerve conduits were listed in Table 1. A porous morphology was observed for both smooth and grooved conduits, and the porosity of all conduits was estimated to be 91% based on Eq. (2). This high porosity of the nerve conduits plays a positive role on nerve regeneration.

Gross Observations and Histological Assessments of Nerve Regeneration

All animals survived the 16-week period following implantation. As shown in Fig. 3a, no gross inflammatory reaction could be observed after nerves had been exposed. The gross observation of *in situ* regenerated nerves showed that these spanned from the proximal to the distal ends of defect gaps in all three

groups (Fig. 3a). An H&E stain was applied to the cross-sectional area of regenerated fibers in the nerve gaps (Fig. 3b). The diameters of the regenerated nerves are shown in Fig. 1d. As can be seen, the diameter of regenerated nerves in the AG group was found to be significantly larger than that of regenerated nerves in the GC and SC groups. Importantly, it was noted that the diameter of regenerated nerves in the GC group was significantly larger compared to that of the SC group.

Images obtained from the immunohistochemical stain are shown in Fig. 3c. Here, the NF200-positive area marks the nerve axons and the GFAP-positive area marks the Schwann cells in the nerve cross-sectional stains. In Fig. 3c, the NF200-positive areas are seen to be more evenly distributed in regenerated nerves of the GC and AG group, indicating an enhanced morphology of the regenerated axons in GC

TABLE 1. The dimensions of nerve conduits.

	Inner grooved conduits	Smooth conduits
Inner diameter (mm)	1.50 ± 0.08	1.46 ± 0.01
Outer diameter (mm)	2.24 ± 0.09	2.24 ± 0.08
Groove height (mm)	0.26 ± 0.02	NA
Groove width (mm)	0.38 ± 0.02	NA
Porosity	91%	91%

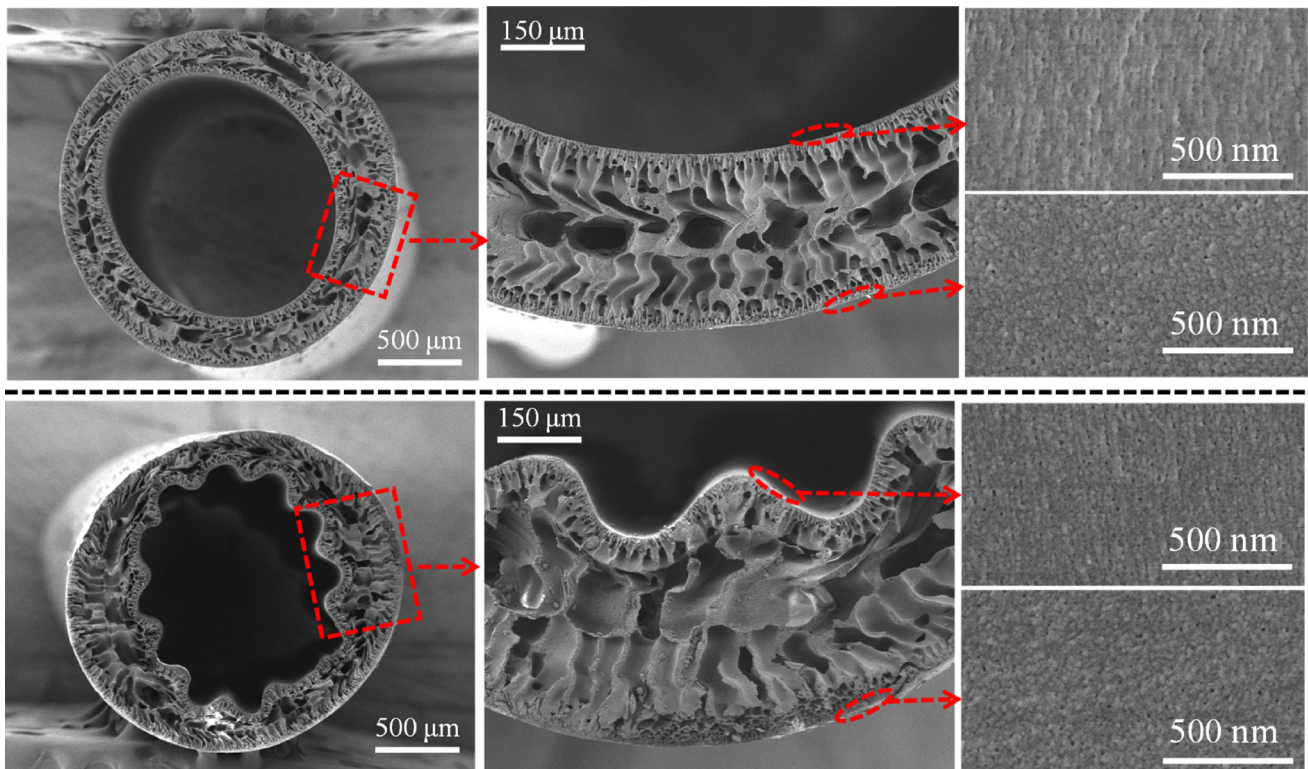


FIGURE 2. SEM images of the cross-sectional, and surface of the smooth and inner grooved nerve conduits.

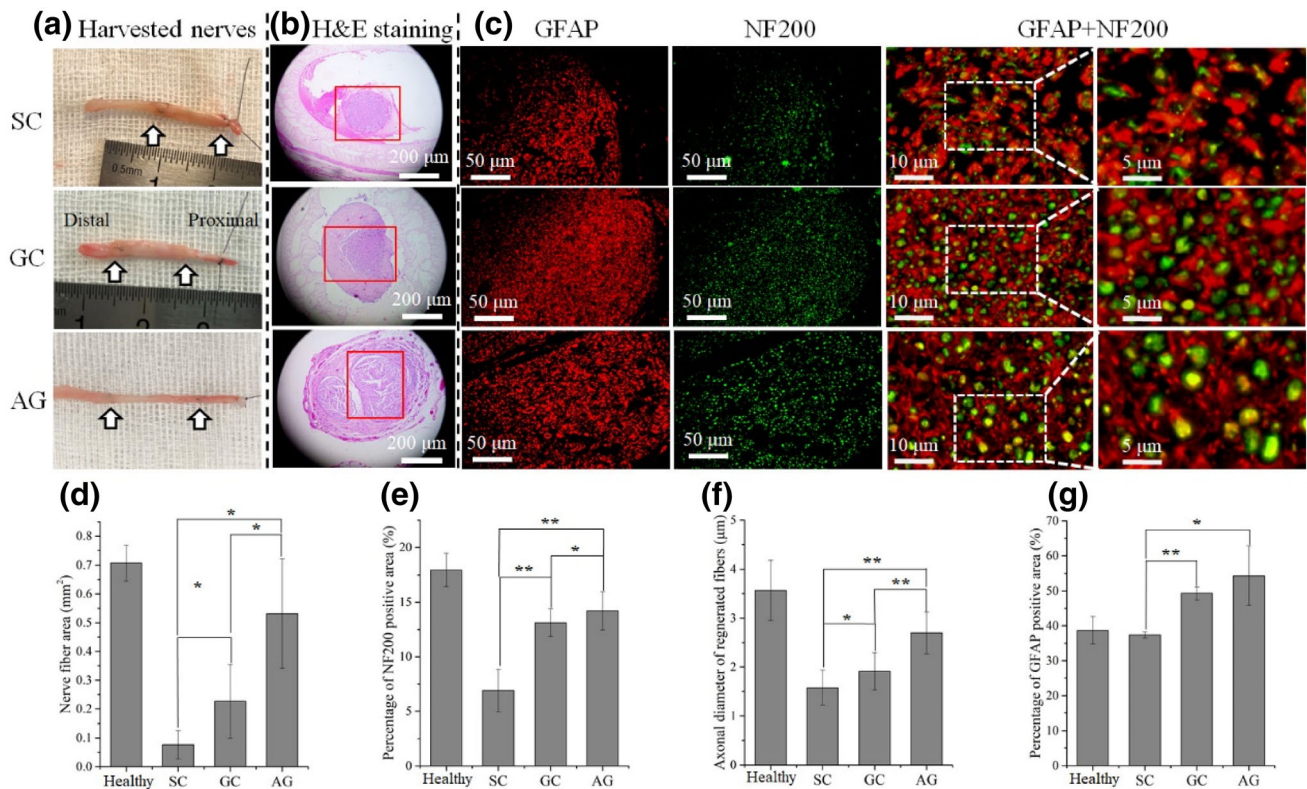


FIGURE 3. Gross observation (a), H&E stain (b), immunohistochemical stain (c), nerve fiber areas (d), percentage of NF200-positive areas (e), axonal diameters of regenerated fibers (f), and percentages of GFAP-positive areas (g). Data are expressed as the mean \pm SD of $n = 5$ per group; * $p < 0.05$ and ** $p < 0.01$.

and AG groups. The ratios of the NF200-positive and GFAP-positive areas were determined to analyze the distribution of regenerated axons and Schwann cells in the recovered nerves. As shown in Figs. 3e and 3f, the ratio of NF200-positive areas was higher in the AG and GC groups than in the SC groups. Additionally, axons in the GC group were seen to show the largest diameter. The AG group showed the highest ratio of GFAP-positive areas (Fig. 3g), with values higher than those seen for the healthy group. The GC group also showed a comparatively high GFAP-positive area ratio which reached a level above the ratio observed for the healthy group and SC group. The enhanced levels of NF200- and GFAP-positive areas in the GC group indicate an improved axon and Schwann cell growth. Furthermore, Schwann cell migration and axon extension were found to be faster in grooved conduits compared to smooth conduits.

TEM Analyses

Since myelination plays a critical role in the rapid transmission of nerve signals, myelin regeneration provides an important base for the assessment of nerve recovery.^{40,45} TEM images of healthy and treated

nerves are shown in Fig. 4a. G-ratios and myelin sheath thickness were determined based on TEM images to evaluate the myelination progression of regenerated nerves. In healthy nerves, myelin sheaths with a circular geometry were observed to show the lowest G-ratios and the highest level of thickness. The AG and GC groups showed low G-ratios and high myelin sheath thickness compared to the SC group (Figs. 4b and 4c). These results indicate an improved remyelination in the GC group in comparison with the SC group.

Thermal Reaction Latency and Electrophysiological Tests

Recovery of sensory function was assessed based on thermal reaction latency tests which can be applied to evaluate the degree of nerve regeneration.²³ Thermal latency data for the treated sites was collected for the different groups. As shown in Fig. 5, the AG group showed the lowest level of reaction latency and the SC group showed the highest level of reaction. Reaction latency in the GC group was seen to be lower than that of the SC group. Based on this, the GC group showed improved motor and sensory function recovery com-

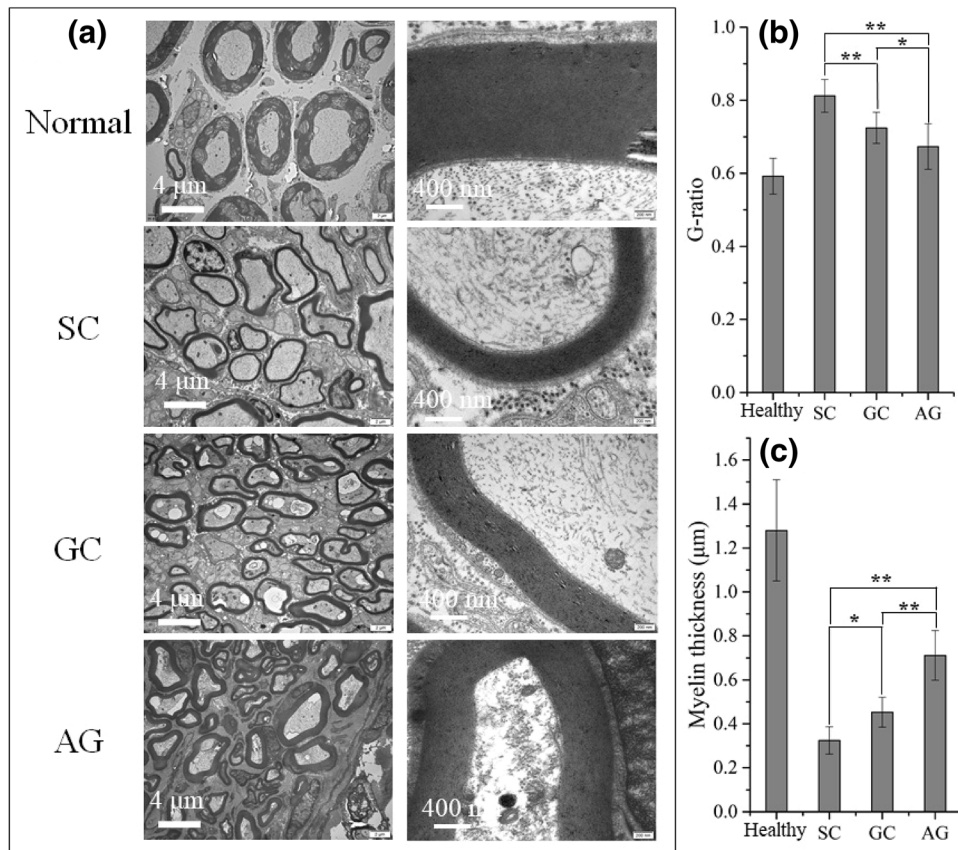


FIGURE 4. TEM images (a), G-ratio data (b), myelin thickness data (c) of healthy and treated nerves. Data are expressed as the mean ± SD of $n = 5$ per group; * $p < 0.05$ and ** $p < 0.01$

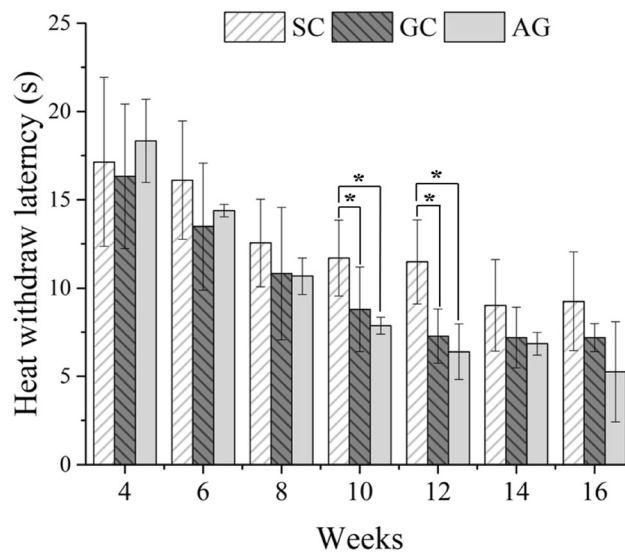


FIGURE 5. Thermal reaction latency test results. Data are expressed as the mean ± SD of $n = 8$ per group; * $p < 0.05$ and ** $p < 0.01$.

pared to the SC group. A significant difference in heat withdrawal latency was observed between the GC and SC groups at the period between week 10 and week 12 post operation. This indicates a rapid recovery of nerve function during these weeks in GC group.

An electrophysiological assessment was carried out to evaluate the functional recovery and reinnervation of regenerated nerves. The recorded CMAPs (Fig. 5), which represent the functional recovery of the target muscles, were utilized to evaluate the level of muscle reinnervation. The CMAP peak amplitude of the AG group was found to be higher than that of both the GC and SC groups, while the CMAP peak amplitude of the GC group was higher than that of the SC group. The CMAP peak amplitude ratio between the treated and the healthy side was calculated (Fig. 6e). The CMAP latency ratio between the treated and healthy side represents an additional quantitative index for the electrophysiological assessment (Fig. 6f). This ratio was found to be the lowest in the AG group and the highest in the SC group. Since a decreased CMAP latency indicates improved functional recovery of the nerve, the GC group showed an enhanced functional reinnervation compared to the SC group.

Gastrocnemius Recovery Evaluation

Nerve injury generally triggers atrophy of the associated gastrocnemius muscle, which leads to muscle weight loss, hyperplasia of connective tissues, and a decrease in muscle size.⁴ During the nerve recovery process, the gastrocnemius muscle undergoes reinnervation. Figure 7a shows the gross images of healthy

gastrocnemii and gastrocnemii extracted from treated nerve injury sites. These results indicated that the volume to which gastrocnemii recovered in the GC group was larger than that observed for the SC group. The wet weight of gastrocnemii in the GC group also showed to be significantly higher than that of gastrocnemii in the SC group (Fig. 7c). To evaluate the level of reinnervation of the target muscle, a Masson's stain was applied. This highlighted the distribution of collagen and muscle fibers in cross-sections of extracted gastrocnemii (Fig. 7b). Here, muscle fibers were stained in red and collagen fibers were stained in blue. It was found that muscle fibers were uniformly distributed in gastrocnemii of the AG, GC and SC groups. The average level of areas containing muscle fibers was found to be significantly higher in the GC group compared to the SC group (Figs. 7d and 7e). These results demonstrate that the level of gastrocnemius recovery in the GC group is similar to the recovery level observed for the AG group.

Regenerated Nerve Morphology and Blood Vessels

In Fig. 8a, the cross-sectional configuration shows that the regenerated nerves inside grooved conduits aligns with the conduits' inner surface topography. While the cross-sectional area of regenerated nerves of smooth conduits in Fig. 8b was much smaller than the nerves of grooved conduits. H&E stains of regenerated nerves and blood vessels in different groups are shown in Figs. 8c–8e. It can be observed that larger quantities of blood vessels were generated in the GC group (Fig. 8c) compared to that in the SC group (Fig. 8d).

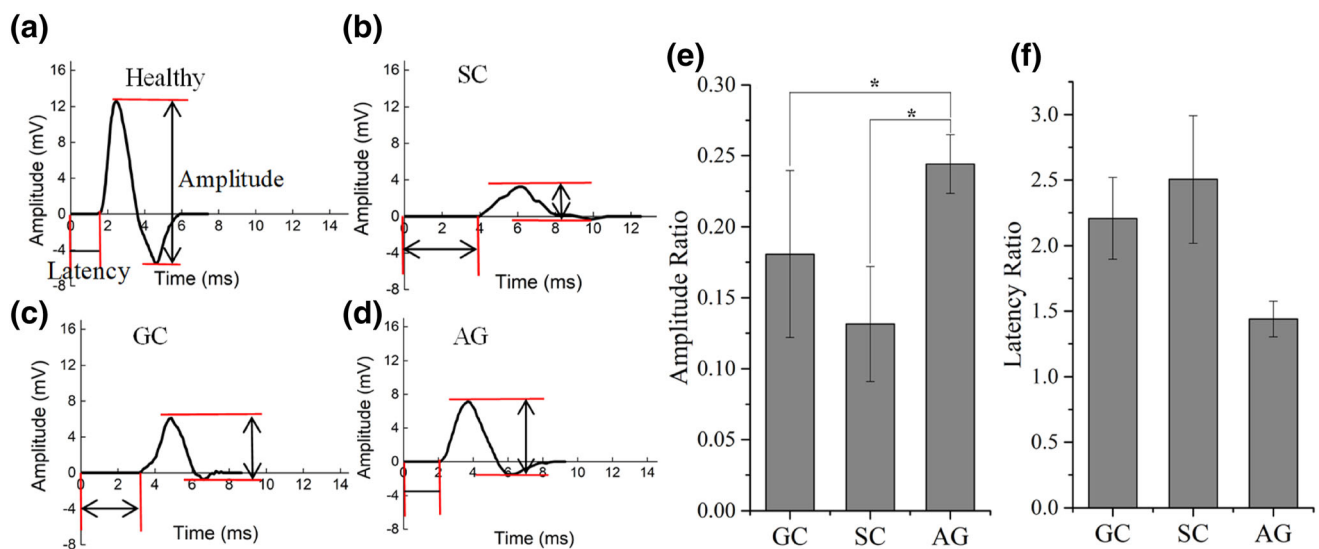


FIGURE 6. Results of electrophysiological tests (a–d), associated CMAP amplitude ratios (e), and CMAP latency ratios (f). Ratios were obtained by dividing values of the treated side data by values of the healthy side data. Data are expressed as the mean \pm SD of $n = 5$ per group; * $p < 0.05$ and ** $p < 0.01$.

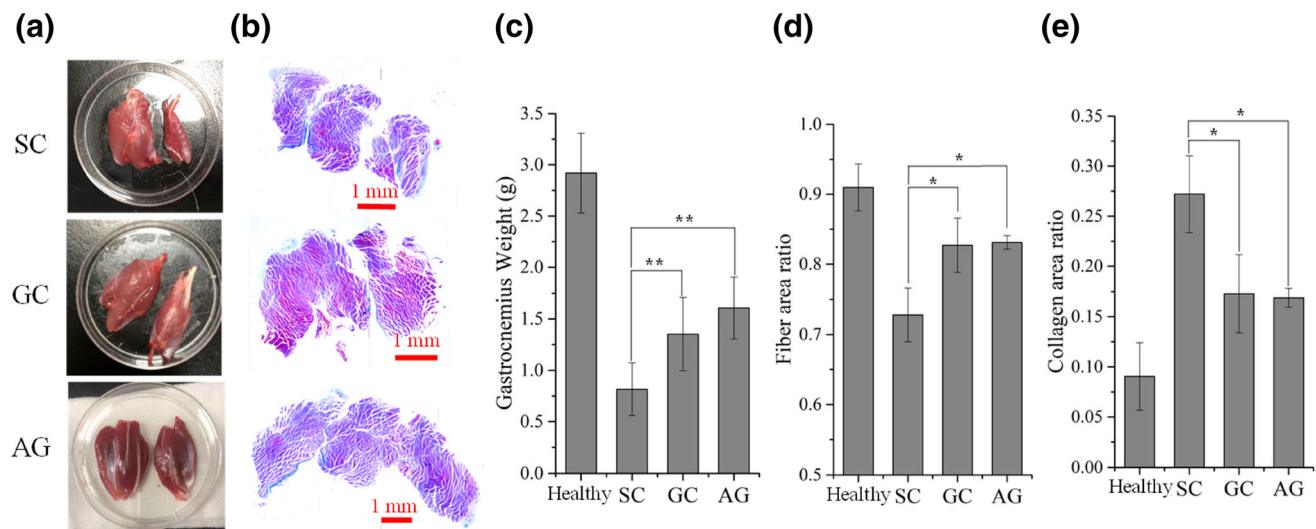


FIGURE 7. (a) Extracted gastrocnemii *in situ*. Left: Gastrocnemii extracted from healthy sides. Right: Gastrocnemii extracted from treated sides. (b) Masson's stain evaluation of gastrocnemii extracted from treated sides. Gastrocnemii recovery evaluation data: (c) gastrocnemii wet weight, (d) gastrocnemii slice muscle fiber area ratios (φ_{muscle}), and (e) gastrocnemii slice collagen fiber area ratios ($\varphi_{\text{collagen}}$). Data are expressed as the mean \pm SD of $n = 8$ per group; * $p < 0.05$ and ** $p < 0.01$.

DISCUSSION

Recently, nerve conduits have been shown to present the basis for an efficient substitute treatment of peripheral nerve injury.^{8,14} Inside the body, the conduits provide a physical template for regenerating nerves.²⁷ Guidance cues such as growth factors can be applied to further improve the efficacy of the nerve conduits.³⁸ Specified groove textures can be used to constrain the growth direction of Schwann cells inside the conduits and to support migration to the target in a pre-designed fashion.⁴¹ Based on the application of conduits, regenerating axons can be guided to reinnervate target muscles while preventing misdirection.⁹ Moreover, the migration speed of Schwann cells has been shown to be increased on grooved surface textures.²⁵ It has also been observed that nerve conduits allow Schwann cells to create a suitable environment for nerve regrowth within a shorter period of time.²⁰ Taken together, these factors can be applied to increase the rate of nerve regeneration and to guide regenerating nerve towards their targets. As a result, the functional loss of affected muscles caused by denervation can be decreased and functional recovery can be improved.¹⁴

The histological analysis (Figs. 3b and 3d) showed that the area of regenerated nerve tissues was larger in the GC group compared to the SC group. This indicates that nerve conduits with an inner grooved surface texture provide enhanced guidance for nerve regeneration. Moreover, PAN is a nondegradable polymer, so the nerve conduits do not degrade during the nerve repair progress. Therefore, the groove textures on the

inner surface showed a good structural stability during the peripheral nerve repair. In Fig. 8a, the alignment of regenerated nerves indicates that the migration of Schwann cells is effectively guided by the conduit grooves. Contrary to the surface area of smooth conduits, the grooved conduits' topography provides a larger contact area for regenerating nerves. This increased surface area is capable of accommodating larger numbers of support cells.⁴ These results are further supported by the finding that the cross-sectional area of regenerating nerves inside smooth conduits was smaller compared to the cross-sectional area of nerves inside grooved conduits (Fig. 8b). The immunohistochemistry results of this study (Figs. 3c and 3g) showed that larger fractions of GFAP-positive areas could be observed in the GC group compared to the SC group. This proves that larger numbers of Schwann cells migrate into grooved conduits, hence leading to improved axonal regeneration, as shown by the NF200-positive areas (Fig. 3c).

H&E stains of regenerated nerves and blood vessels in different groups are shown in Figs. 8c–8e. Larger numbers of blood vessels in regenerating nerves contribute to an enhanced nutrient supply and provide a preferred environment for axonal sprouting and growth.^{7,21} Recent studies have also shown that regenerating blood vessels can guide the migration of Schwann cells and other cell types inside nerve gaps.² In Figs. 8c–8e, it can be observed that larger quantities of blood vessels were generated in the GC group (Fig. 8c) compared to the SC group (Fig. 8d).

The goal of this study was to introduce a longitudinally aligned grooved texture on the inner surface of

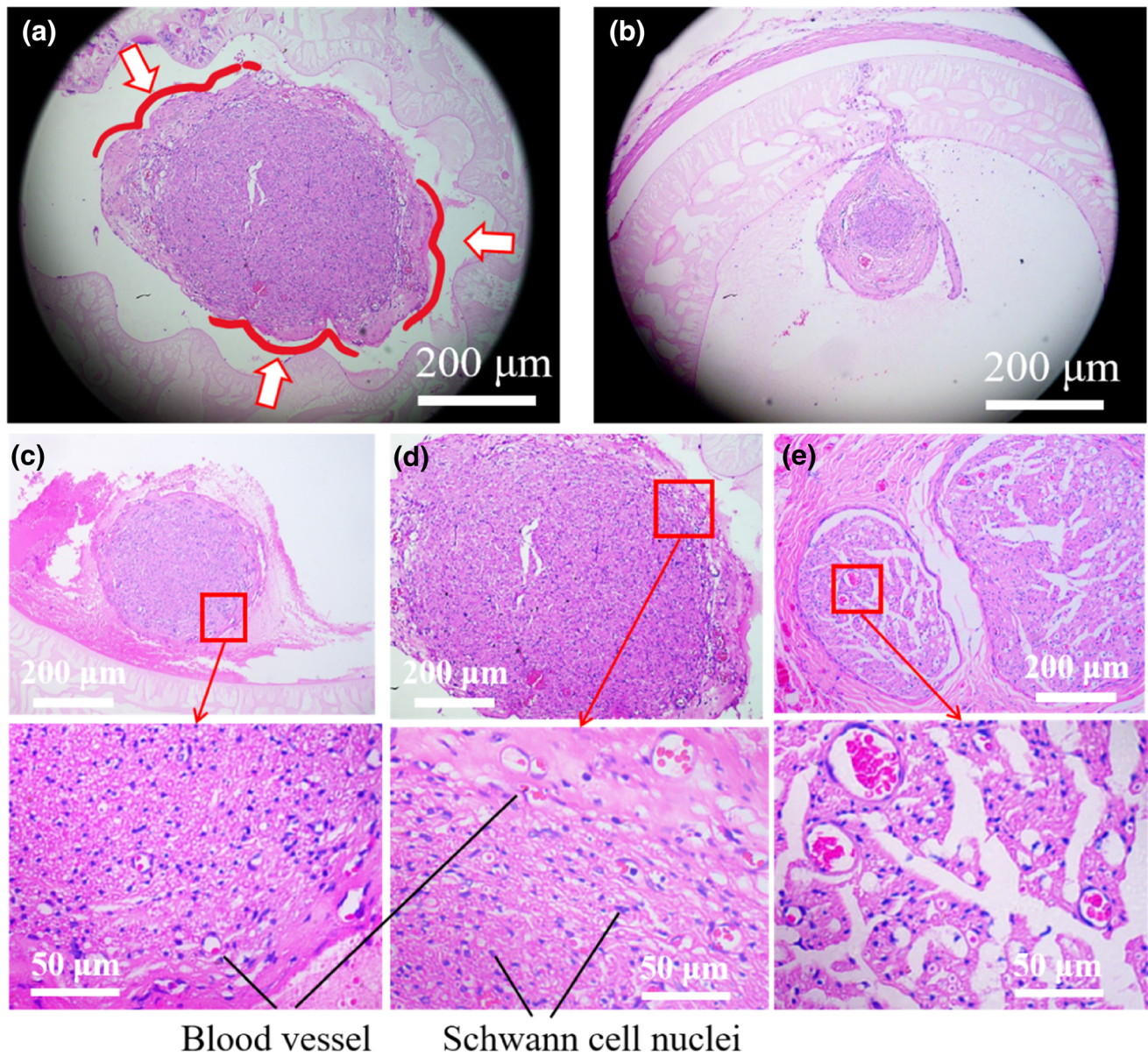


FIGURE 8. Nerve fibers growing along grooved (a) and smooth (b) conduits. Red arrows mark cross-sectional shapes of nerves guided by grooved textures. Blood vessels and Schwann cells in the SC (c), GC (d), and AG (e) groups are highlighted by an H&E stain.

polymeric nerve conduits to provide physical guidance cues for improved peripheral nerve injury repair. The experimental results of this *in vivo* study indicate a significant enhancement of rat sciatic nerve regeneration based on the application of grooved PAN nerve conduits. This level of regeneration could not be seen for smooth PAN nerve conduits. Based on experimental observations, several features of the conduits' inner grooved texture may contribute to the enhancement of peripheral nerve recovery. First, the grooved texture can restrict neuronal extension and axon outgrowth due to the limited flexibility of the cell cytoplasm.³⁵ The open lumen inside the nerve conduits

does, however, provide the space required for cell–cell interactions during nerve regeneration. Second, the grooved texture offers an increased level of surface area. The resulting increase in surface-area-to-volume-ratio facilitates cell adhesion. A larger surface area also provides benefits for the diffusion of waste products and nutrients. It, hence, contributes to the formation of a supportive environment for cell growth.⁵¹

In the future, the fundamental mechanisms which underlie the groove guidance effects on regenerating nerve tissues should be carefully studied. This will aid the optimization of grooved inner textures inside nerve conduits. Furthermore, the repair efficiency of these

conduits may be further improved by combining different physical and/or biological guidance cues, such as electrical stimulation, nerve growth factors and stem cells.³⁹

In this study, PAN nerve conduits with inner grooved textures were prepared using the dry-jet wet spinning method. The generated nerve conduits were implanted into SD rats to bridge 10 mm sciatic nerve gaps. Behavioral, electrophysiological, histological and immunohistochemical tests were applied to evaluate the effects of the conduits' grooved inner patterns on nerve repair. Nerves treated with grooved conduits showed improved outcomes compared to nerves treated with smooth conduits, as these showed enhanced results for behavioral reactions, electrophysiological functions, nerve fiber diameters, levels of remyelinated axons, Schwann cell quantities, and muscle recovery. In contrast to the SC group, the GC group showed larger areas of regenerated nerves and increased quantities of blood. The outcomes of this study prove that PAN nerve conduits with grooved inner guidance structures of ~200–300 μm significantly enhance peripheral nerve recovery.

ACKNOWLEDGMENTS

Authors sincerely thank Chaonan Yu for preparing and housing SD rats. This study was partially supported by the National Key Research and Development Program of China (Grant No. 2018YFA0703000), the Key Research and Development Program of Zhejiang Province (Grant No. 2017C01063), the Science Fund for Creative Research Groups of the National Natural Science Foundation of China (Grant No. 51821093), the National Natural Science Foundation of China (Grant No. U1609207, 81873911), the Public Projects of Zhejiang Province (Grant No. 2019C03033), the Zhejiang Medical Science and Technology Project (Grant No. 2019KY569), and the Natural Foundation of Ningbo (Grant No. 2017A610215).

REFERENCES

- ¹Beigi, M. H., L. Ghasemi-Mobarakeh, M. P. Prabhakaran, K. Karbalaie, H. Azadeh, S. Ramakrishna, H. Baharvand, and M. H. Nasr-Esfahani. In vivo integration of poly (ϵ -caprolactone)/gelatin nanofibrous nerve guide seeded with teeth derived stem cells for peripheral nerve regeneration. *J. Biomed. Mater. Res. Part A* 102:4554–4567, 2014.
- ²Cattin, A., J. J. Burden, L. Van Emmenis, F. E. Mackenzie, J. J. Hoving, N. G. Calavia, Y. Guo, M. McLaughlin, L. H. Rosenberg, V. Quereda, D. Jamecna, I. Napoli, S. Parrinello, T. TariqEnver, C. Ruhrberg, and A. C. Lloyd. Macrophage-induced blood vessels guide schwann cell-mediated regeneration of peripheral nerves. *Cell* 162:1127–1139, 2015.
- ³Chang, Y., M. Chen, S. Liao, H. Wu, C. Kuan, J. Sun, and T. Wang. Multichanneled nerve guidance conduit with spatial gradients of neurotrophic factors and oriented nanotopography for repairing the peripheral nervous system. *ACS Appl. Mater. Interfaces*. 9:37623–37636, 2017.
- ⁴Chang, W., M. B. Shah, P. Lee, and X. Yu. Tissue-engineered spiral nerve guidance conduit for peripheral nerve regeneration. *Acta Biomater.* 73:302–311, 2018.
- ⁵Chua, J. S., C. P. Chng, A. A. K. Moe, J. Y. Tann, E. L. Goh, K. H. Chiam, and E. K. Yim. Extending neurites sense the depth of the underlying topography during neuronal differentiation and contact guidance. *Biomaterials* 35:7750–7761, 2014.
- ⁶Daly, W., L. Yao, D. Zeugolis, A. Windebank, and A. Pandit. A biomaterials approach to peripheral nerve regeneration: bridging the peripheral nerve gap and enhancing functional recovery. *J. R. Soc. Interface*. 9:202–221, 2011.
- ⁷Dray, C., G. Rougon, and F. Debarbieux. Quantitative analysis by in vivo imaging of the dynamics of vascular and axonal networks in injured mouse spinal cord. *Proc. Natl. Acad. Sci.* 106:9459–9464, 2009.
- ⁸Farokhi, M., F. Mottaghitalab, M. A. Shokrgozar, D. L. Kaplan, H. Kim, and S. C. Kundu. Prospects of peripheral nerve tissue engineering using nerve guide conduits based on silk fibroin protein and other biopolymers. *Int. Mater. Rev.* 62:367–391, 2017.
- ⁹Faroni, A., S. A. Mobasser, P. J. Kingham, and A. J. Reid. Peripheral nerve regeneration: experimental strategies and future perspectives. *Adv. Drug Deliv. Rev.* 82:160–167, 2015.
- ¹⁰Gaudin, R., C. Knipfer, A. Henningsen, R. Smeets, M. Heiland, and T. Hadlock. Approaches to peripheral nerve repair: generations of biomaterial conduits yielding to replacing autologous nerve grafts in craniomaxillofacial surgery. *Int BioMed Res* 2016. <https://doi.org/10.1155/2016/3856262>.
- ¹¹Gill, E. L., X. Li, M. A. Birch, and Y. Y. S. Huang. Multi-length scale bioprinting towards simulating microenvironmental cues. *Bio-des. Manuf.* 1:77–88, 2018.
- ¹²Gordon, T., and G. H. Borschel. The use of the rat as a model for studying peripheral nerve regeneration and sprouting after complete and partial nerve injuries. *Exp. Neurol.* 287:331–347, 2017.
- ¹³Grinberg, Y., M. A. Schiefer, D. J. Tyler, and K. J. Gustafson. Fascicular perineurium thickness, size, and position affect model predictions of neural excitation. *IEEE Trans. Neural Syst. Rehabil. Eng.* 16:572–581, 2008.
- ¹⁴Grinsell, D., and C. P. Keating. Peripheral nerve reconstruction after injury: a review of clinical and experimental therapies. *BioMed Res. Int.* 13:698256–698256, 2014. <http://doi.org/10.1155/2014/698256>.
- ¹⁵Gu, X., F. Ding, Y. Yang, and J. Liu. Construction of tissue engineered nerve grafts and their application in peripheral nerve regeneration. *Prog. Neurobiol.* 93:204–230, 2011.
- ¹⁶Guo, Q., C. Liu, B. Hai, T. Ma, W. Zhang, J. Tan, X. Fu, H. Wang, Y. Xu, and C. Song. Chitosan conduits filled with simvastatin/Pluronic F-127 hydrogel promote

- peripheral nerve regeneration in rats. *J. Biomed. Mater. Res. Part B* 106:787–799, 2018.
- ¹⁷Hoffman-Kim, D., J. A. Mitchel, and R. V. Bellamkonda. Topography, cell response, and nerve regeneration. *Annu. Rev. Biomed. Eng.* 12:203–231, 2010.
- ¹⁸Holland, I., J. Logan, J. Shi, C. McCormick, D. Liu, and W. Shu. 3D biofabrication for tubular tissue engineering. *Bio-des. Manuf.* 1:89–100, 2018.
- ¹⁹Hsu, S., C. Chen, P. S. Lu, C. Lai, and C. Chen. Oriented Schwann cell growth on microgrooved surfaces. *Biotechnol. Bioeng.* 92:579–588, 2005.
- ²⁰Hsu, S., P. S. Lu, H. Ni, and C. Su. Fabrication and evaluation of microgrooved polymers as peripheral nerve conduits. *Biomed. Microdevices* 9:665–674, 2007.
- ²¹Hsu, S. H., and H. C. Ni. Fabrication of the microgrooved/microporous polylactide substrates as peripheral nerve conduits and in vivo evaluation. *Tissue Eng. Part A* 15:1381–1390, 2008.
- ²²Huang, C., Y. Ouyang, H. Niu, N. He, Q. Ke, X. Jin, D. Li, J. Fang, W. Liu, C. Fan, and T. Lin. Nerve guidance conduits from aligned nanofibers: improvement of nerve regeneration through longitudinal nanogrooves on a fiber surface. *ACS Appl. Mater. Interfaces* 7:7189–7196, 2015.
- ²³Jin, J., S. Limburg, S. K. Joshi, R. Landman, M. Park, Q. Zhang, H. T. Kim, and A. C. Kuo. Peripheral nerve repair in rats using composite hydrogel-filled aligned nanofiber conduits with incorporated nerve growth factor. *Tissue Eng. Part A* 19:2138–2146, 2013.
- ²⁴Johnson, B. N., K. Z. Lancaster, G. Zhen, J. He, M. K. Gupta, Y. L. Kong, E. A. Engel, K. D. Krick, A. Ju, F. Meng, L. W. Enquist, X. Jia, and M. C. Mcalpine. 3D printed anatomical nerve regeneration pathways. *Adv. Funct. Mater.* 25:6205–6217, 2015.
- ²⁵Kim, S. M., M. S. Lee, J. Jeon, D. H. Lee, K. Yang, S. Cho, I. Han, and H. S. Yang. Biodegradable nerve guidance conduit with microporous and micropatterned poly(lactic-co-glycolic acid)-accelerated sciatic nerve regeneration. *Macromol. Biosci.* 18:1800290, 2018.
- ²⁶Krych, A. J., G. E. Rooney, B. Chen, T. C. Schermerhorn, S. Ameenuddin, L. Gross, M. J. Moore, B. L. Currier, R. J. Spinner, J. A. Friedman, M. J. Yaszemski, and A. J. Windebank. Relationship between scaffold channel diameter and number of regenerating axons in the transected rat spinal cord. *Acta Biomater.* 5:2551–2559, 2009.
- ²⁷Lackington, W. A., A. J. Ryan, and F. J. Brien. Advances in nerve guidance conduit-based therapeutics for peripheral nerve repair. *ACS Biomater. Sci. Eng.* 3(1221–1235):2017, 2017.
- ²⁸Li, C. W., B. Davis, J. Shea, H. Sant, B. K. Gale, and J. Agarwal. Optimization of micropatterned poly (lactic-co-glycolic acid) films for enhancing dorsal root ganglion cell orientation and extension. *Neural Regener. Res.* 13:105, 2018.
- ²⁹Long, Y., N. Zhang, Y. Huang, and X. Wen. Formation of highly aligned grooves on inner surface of semipermeable hollow fiber membrane for directional axonal outgrowth. *J. Manuf. Sci. Eng.* 130:021011, 2008.
- ³⁰Ma, T., L. Zhu, Y. Yang, X. Quan, L. Huang, Z. Liu, Z. Sun, S. Zhu, J. Huang, and Z. Luo. Enhanced in vivo survival of Schwann cells by a synthetic oxygen carrier promotes sciatic nerve regeneration and functional recovery. *J. Tissue Eng. Regen. Med.* 12:e177–e189, 2018.
- ³¹Mobasserri, A., A. Faroni, B. M. Minogue, S. Downes, G. Terenghi, and A. J. Reid. Polymer Scaffolds with preferential parallel grooves enhance nerve regeneration. *Tissue Eng. Part A* 21:1152–1162, 2015.
- ³²Nectow, A. R., K. G. Marra, and D. L. Kaplan. Biomaterials for the development of peripheral nerve guidance conduits. *Tissue Eng. Part B* 18:40–50, 2012.
- ³³Nguyen, A. T., S. R. Sathe, and E. K. Yim. From nano to micro: topographical scale and its impact on cell adhesion, morphology and contact guidance. *J. Phys.* 28:183001, 2016.
- ³⁴Oh, S. H., J. G. Kang, T. H. Kim, U. Namgung, K. S. Song, B. H. Jeon, and J. H. Lee. Enhanced peripheral nerve regeneration through asymmetrically porous nerve guide conduit with nerve growth factor gradient. *J. Biomed. Mater. Res. Part A* 106:52–64, 2018.
- ³⁵Pawelec, K. M., J. Koffler, D. Shahriari, A. R. Galvan, M. H. Tuszynski, and J. Sakamoto. Microstructure and in vivo characterization of multi-channel nerve guidance scaffolds. *Biomed. Mater.* 13:044104, 2018.
- ³⁶Quan, Q., H. Y. Meng, B. Chang, G. B. Liu, X. Q. Cheng, H. Tang, Y. Wang, J. Peng, Q. Zhao, and S. B. Lu. Aligned fibers enhance nerve guide conduits when bridging peripheral nerve defects focused on early repair stage. *Neural Regener. Res.* 14:903, 2019.
- ³⁷Roach, P., T. Parker, N. Gadegaard, and M. R. Alexander. Surface strategies for control of neuronal cell adhesion: a review. *Surf. Sci. Rep.* 65:145–173, 2010.
- ³⁸Sarker, M., S. Naghieh, A. D. McInnes, D. J. Schreyer, and X. B. Chen. Strategic design and fabrication of nerve guidance conduits for peripheral nerve regeneration. *Biotechnol. J.* 13:1700635, 2018.
- ³⁹Sarker, M. D., S. Naghieh, A. D. McInnes, D. J. Schreyer, and X. B. Chen. Regeneration of peripheral nerves by nerve guidance conduits: influence of design, biopolymers, cells, growth factors, and physical stimuli. *Prog. Neurobiol.* 171:125–150, 2018.
- ⁴⁰Seidl, A. H. Regulation of conduction time along axons. *Neuroscience* 276:126–134, 2014.
- ⁴¹Simitzi, C., A. Ranella, and E. Stratakis. Controlling the morphology and outgrowth of nerve and neuroglial cells: the effect of surface topography. *Acta Biomater.* 51:21–52, 2017.
- ⁴²Suo, H., Z. Wang, G. Dai, J. Fu, J. Yin, and L. Chang. Polyacrylonitrile nerve conduits with inner longitudinal grooved textures to enhance neuron directional outgrowth. *IEEE/ASME J. Microelectromech. Syst.* 27:457–463, 2018.
- ⁴³Tao, J., Y. Hu, S. Wang, J. Zhang, X. Liu, Z. Gou, H. Cheng, Q. Liu, Q. Zhang, S. You, and M. Gou. A 3D-engineered porous conduit for peripheral nerve repair. *Sci. Rep.* 7(1):46038, 2017.
- ⁴⁴Tao, J., J. Zhang, T. Du, X. Xu, X. Deng, S. Chen, J. Liu, Y. Chen, X. Liu, M. Xiong, Y. Luo, H. Cheng, J. Mao, L. Cardon, M. Gou, and Y. Wei. Rapid 3D printing of functional nanoparticle-enhanced conduits for effective nerve repair. *Acta Biomater.* 90:49–59, 2019.
- ⁴⁵Vleggeert-Lankamp, C. L. The role of evaluation methods in the assessment of peripheral nerve regeneration through synthetic conduits: a systematic review. *J. Neurosurg.* 107:1168–1189, 2007.
- ⁴⁶Wang, Y., W. Wang, Y. Wo, T. Gui, H. Zhu, X. Mo, C. Chen, Q. Li, and W. Ding. Orientated guidance of peripheral nerve regeneration using conduits with a microtube array sheet (MTAS). *ACS Appl. Mater. Interfaces* 7:8437–8450, 2015.
- ⁴⁷Wen, X., and P. A. Tresco. Effect of filament diameter and extracellular matrix molecule pre-coating on neurite out-

- growth and Schwann cell behavior on multifilament entubulation bridging device in vitro. *J. Biomed. Mater. Res., Part A* 76:626–637, 2006.
- ⁴⁸Xu, X., J. Tao, S. Wang, L. Yang, J. Zhang, J. Zhang, H. Liu, H. Cheng, J. Xu, M. Gou, and Y. Wei. 3D printing of nerve conduits with nanoparticle-encapsulated RGFP966. *Appl. Mater. Today* 16:247–256, 2019.
- ⁴⁹Yao, L., S. Wang, W. Cui, R. Sherlock, C. O’Connell, G. Damodaran, A. Gorman, A. Windebank, and A. Pandit. Effect of functionalized micropatterned PLGA on guided neurite growth. *Acta Biomater.* 5:580–588, 2009.
- ⁵⁰Yin, J., Z. Wang, W. Chai, G. Dai, H. Suo, N. Zhang, X. Wen, and Y. Huang. Fabrication of inner grooved hollow fiber membranes using microstructured spinneret for nerve regeneration. *J. Manuf. Sci. Eng.* 139:111007, 2017.
- ⁵¹Zhao, Y., Q. Zhang, L. Zhao, L. Gan, L. Yi, Y. Zhao, J. Xue, L. Luo, Q. Du, R. Geng, Z. Sun, N. Benkirane-Jessel, P. Chen, and Y. Li. Enhanced peripheral nerve regeneration by a high surface area to volume ratio of nerve conduits fabricated from hydroxyethyl cellulose/soy protein composite sponges. *ACS Omega.* 2:7471–7481, 2017.
- ⁵²Zhong, Y., L. Wang, J. Dong, Y. Zhang, P. Luo, J. Qi, X. Liu, and C. J. Xian. Three-dimensional reconstruction of peripheral nerve internal fascicular groups. *Sci. Rep.* 5:17168–17168, 2015.
- ⁵³Zhu, S., J. Ge, Y. Wang, F. Qi, T. Ma, M. Wang, Y. Yang, Z. Liu, J. Huang, and Z. Luo. A synthetic oxygen carrier-olfactory ensheathing cell composition system for the promotion of sciatic nerve regeneration. *Biomaterials* 35:1450–1461, 2014.

Publisher’s Note Springer Nature remains neutral with regard to jurisdictional claims in published maps and institutional affiliations.